0022-3565/07/3222-709–720$20.00
THE JOURNAL OF PHARMACOLOGY AND EXPERIMENTAL THERAPEUTICS
Vol. 322, No. 2
123000/3231401
JPET 322:709–720, 2007
Printed in U.S.A.

Identification and Characterization of Cholest-4-en-3-one, Oxime (TRO19622), a Novel Drug Candidate for Amyotrophic Lateral Sclerosis[S]

Thierry Bordet, Bruno Buisson, Magali Michaud, Cyrille Drouot, Pascale Galéa, Pierre Delaage, Natalia P. Akentieva, Alex S. Evers, Douglas F. Covey, Mariano A. Ostuni, Jean-Jacques Lacapère, Charbel Massaad, Michael Schumacher, Esther-Marie Steidl, Delphine Maux, Michel Delaage, Christopher E. Henderson,[1] and Rebecca M. Pruss

Trophos, Parc Scientifique de Luminy case 931, Marseille, France (T.B., B.B., M.M., C.D., P.G., P.D., E.-M.S., D.M., M.D., R.M.P.); Washington University School of Medicine, St. Louis, Missouri (N.P.A., A.S.E., D.F.C.); U773 Institut National de la Santé et de la Recherche Médicale, Centre de Recherche Biologique Bichat Beaujeon (CRB3), Université Paris 7, Faculté de Médecine Bichat, Paris, France (M.A.O., J.-J.L.); Unité Mixte de Recherche 788, Institut National de la Santé et de la Recherche Médicale, Université Paris 11, Le Kremlin-Bicêtre, France (C.M., M.S.); and Unité Mixte de Recherche 623, Institut National de la Santé et de la Recherche Médicale, Parc Scientifique de Luminy, Marseille, France (C.E.H.)

Received March 20, 2007; accepted May 10, 2007

ABSTRACT

Amyotrophic lateral sclerosis (ALS) is a fatal neurodegenerative disorder characterized by progressive death of cortical and spinal motor neurons, for which there is no effective treatment. Using a cell-based assay for compounds capable of preventing motor neuron cell death in vitro, a collection of approximately 40,000 low-molecular-weight compounds was screened to identify potential small-molecule therapeutics. We report the identification of cholest-4-en-3-one, oxime (TRO19622) as a potential drug candidate for the treatment of ALS. In vitro, TRO19622 promoted motor neuron survival in the absence of trophic support in a dose-dependent manner. In vivo, TRO19622 rescued motor neurons from axotomy-induced cell death in neonatal rats and promoted nerve regeneration following sciatic nerve crush in mice. In SOD1^{G93A} transgenic mice, a model of familial ALS, TRO19622 treatment improved motor performance, delayed the onset of the clinical disease, and extended survival. TRO19622 bound directly to two components of the mitochondrial permeability transition pore: the voltage-dependent anion channel and the translocator protein 18 kDa (or peripheral benzodiazepine receptor), suggesting a potential mechanism for its neuroprotective activity. TRO19622 may have therapeutic potential for ALS and other motor neuron and neurodegenerative diseases.

Amyotrophic lateral sclerosis (ALS) is a rapidly progressive neurodegenerative disorder that selectively affects motor neurons in the spinal cord, brainstem, and cortex. ALS affects people of all races and ethnic backgrounds with an incidence approximately 2 per 100,000 individuals (McGuire and Nelson, 2006). The onset of ALS is most common in the 55 to 75 year age range, and incidence rises with advancing age; men have a higher risk of developing the disease than women (Nelson, 1995). Common clinical features of ALS include muscle weakness and fasciculations. These occur predominantly in limbs, although bulbar onset pathology can also lead to tongue atrophy and dysphagia. Failure of the respiratory muscles and cardiac complications are generally the fatal event, occurring within an average of 3 years of disease onset, with only a 5% chance of survival 5 years after diagnosis (del Aguila et al., 2003). Although 5 to 10% of ALS

This work was supported by the Association Française contre les Myopathies.
[1] Current affiliation: Center for Motor Neuron Biology and Disease, Columbia University, New York.
Article, publication date, and citation information can be found at http://jpet.aspetjournals.org.
doi:10.1124/jpet.107.123000.
[S] The online version of this article (available at http://jpet.aspetjournals.org) contains supplemental material.

ABBREVIATIONS: ALS, amyotrophic lateral sclerosis; SOD, superoxide dismutase; TRO19622, cholest-4-en-3-one, oxime; CsA, cyclosporine A; DMSO, dimethyl sulfoxide; AM, acetoxymethyl ester; PK11195, 1-(2-chlorophenyl)-*N*-methyl-*N*-(1-methyl-propyl)-3-isoquinoline carboxamide; TSPO, translocator protein 18 kDa; VDAC, voltage-dependent anion channel; 6-AziP, 6-azi-3α-hydroxy-5β-pregnan-20-one; CGC, cerebellar granule cell; PR, progesterone receptor; CMAP, compound muscle action potential; mPTP, mitochondrial permeability transition pore; R-5020, 17α,21-dimethyl-19-nor-4,9-pregnadiene-3,20-dione; h, human; 3α5β-TH PROG, 3α-hydroxy-5β-pregnan-20-one; 3α5α-TH PROG, 3α-hydroxy-5α-pregnan-20-one.

cases are inherited, most cases are sporadic and the underlying causes of the disease remain unknown. Riluzole, currently the only drug approved for the treatment of ALS, prolongs survival by 2 to 3 months without improvement in motor functions (Bensimon et al., 1994); therefore, new therapies are urgently needed.

Some clues to the pathogenesis of ALS have come from the discovery of >100 mutations in the gene coding for superoxide dismutase SOD1; these mutations are responsible for 20% of familial cases of ALS. These mutations lead to a toxic gain of function, and they do not necessarily affect enzyme activity. Abnormal protein folding leading to aggregation, inappropriate targeting to mitochondria, and increased free radical generation are considered to be potential mediators triggering neuronal dysfunction and ultimately death (Bendotti and Carri, 2004; Bruijn et al., 2004). Oxidative stress and mitochondrial dysfunction can make cells vulnerable to excitotoxicity due to loss of calcium-buffering capacity and/or ATP depletion. Even though SOD1 mutations are found in only a small subset of ALS patients, the dysfunction triggered by these mutations may underlie sporadic cases as well.

During the ALS disease process, loss of neuromuscular connections through dying back of axons is followed by programmed cell death of motor neurons (for review, see Sathasivam and Shaw, 2005). Neurotrophic factors promote both motor neuron survival and growth during development (Oppenheim, 1989). These factors rescue spinal motor neurons from axotomy-induced cell death (Sendtner et al., 1990), and they accelerate regeneration of motor axons after nerve lesion in rodents (Friedman et al., 1995), suggesting that motor neuron disease might benefit from neurotrophic factor administration (Henderson, 1995). Indeed, when administered to animal models, by cellular or gene therapy, neurotrophic factors were effective in slowing motor neuron degeneration (Sendtner et al., 1992; Haase et al., 1999; Bordet et al., 2001; Lesbordes et al., 2003). However, clinical trials of trophic factors failed to demonstrate efficacy, probably due to the poor absorption, distribution, and metabolic properties of these polypeptides (Apfel, 2001). Interest has therefore turned toward identifying small molecules that can mimic trophic factors and support motor neuron survival and thereby treat motor neuron diseases.

In the absence of validated targets or a clear understanding of the pathogenesis of ALS, we developed a phenotypic cell-based screening approach, selecting motor neuron survival as a clinically relevant endpoint. We took advantage of techniques for purifying and culturing motor neurons from embryonic rat spinal cord (Henderson et al., 1995). These cultured motor neurons retain several key properties of motor neurons in vivo, including dependence on trophic factors for survival. Indeed, approximately 15 different motor neuron trophic factors have been identified using purified motor neurons as a bioassay (Oppenheim, 1996). Here, we report that small chemical compounds can have similar properties. TRO19622 is a small molecule that displays remarkable neuroprotective and neuroregenerative properties for motor neurons in vitro and in several animal models of neurodegeneration and nerve trauma. It is therefore a promising candidate for development to treat ALS and other motor neuron diseases such as spinal muscular atrophy.

Materials and Methods

Drugs. TRO19622 (Fig. 1) was synthesized by Archemis (Décines Charpieu, France). Cyclosporin A (CsA) was purchased from Sigma-Aldrich (St. Louis, MO). For in vitro studies, TRO19622 was dissolved in dimethyl sulfoxide (DMSO) to prepare 10^{-2} M stock solutions that were diluted to their final concentration in the appropriate buffer or medium. For in vivo studies, TRO19622 was administrated either by oral gavage as a suspension in hydroxypropylmethylcellulose or vegetable oil or by subcutaneous injection for long-term studies as a solution in a mixture of Cremophor EL/DMSO/ethanol/phosphate-buffered saline (5:5:10:80, respectively).

Animals. Sprague-Dawley rat embryos or newborn pups (Elevage Janvier, Le Genest Saint Isle, France) were used for in vitro neuronal assays or facial nerve axotomy, respectively. Adult female C57bl/6 RJ mice (Charles River Laboratories, L'Arbresle, France) were used for sciatic nerve regeneration studies. Animals were maintained in a room with controlled temperature (21–22°C) and a reverse 12-h light/dark cycle with food and water available ad libitum. All experiments were carried out in accordance with European legislation and institutional operating procedures.

Motor Neuron Trophic Deprivation Model. Motor neurons were prepared from embryonic day 14 rat spinal cord to ~95% purity using a two-step density centrifugation and immunopurification procedure as described previously (Henderson et al., 1995). Purified motor neurons were seeded at 530 cells/well in polyornithine/laminin-coated 96-well plates in Neurobasal medium supplemented with 2% B-27 (Invitrogen, Carlsbad, CA), 25 μM 2-mercaptoethanol, and 2% horse serum. Test substances were added 1 h after plating. TRO19622 was added to final concentrations ranging from 0.1 to 10 μM in 0.1% DMSO (n = 8 wells/concentration). A cocktail of neurotrophic factors (1 ng/ml brain-derived neurotrophic factor, 10 ng/ml ciliary neurotrophic factor, and 1 ng/ml glia-derived neurotrophic factor) was used as a positive control, and it was defined as 100% survival, whereas survival in basal medium (i.e., without trophic factors) was defined as 0% survival (negative control). After 3 days of culture, surviving motor neurons were stained using a vital dye, calcein-AM (Invitrogen) at 2 μg/ml for 30 min. Next, fluorescence of the medium was quenched with 5 mg/ml hemoglobin, and cell survival was determined by direct and automatic counting of fluorescent motor neurons using the Flash Cytometer (Supplemental Fig. 1), a fluorescence imaging plate reader developed for this task by Trophos (Marseilles, France).

Automated Measurement of Motor Neuron Survival and Neurite Outgrowth. Motor neuron cultures were stained with calcein-AM, and automatic image acquisition of all cells in individual wells of a 96-well plate was performed using the Flash Cytometer. Cell survival was automatically quantified in each well using dedicated software (Tina version 4.8; Trophos). Measurement of neurite outgrowth was next performed with MetaMorph Neurite Outgrowth Application Module (Molecular Devices, Sunnyvale, CA). Classification for cell bodies and outgrowth were optimized following the manufacturer's instructions and by comparing the image using MetaMorph with the original image from the Flash Cytometer. Total cell number, neurite outgrowth/cell, number of processes, and branches/cell were then calculated automatically for all cells present in an entire well of a 96-well plate.

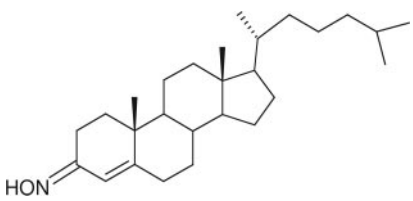

Fig. 1. Chemical structure of TRO19622. TRO19622 exists as a stable mixture of syn- and anti-isomers of cholest-4-en-3-one, oxime.

Nuclear Steroid Receptors. The affinity of TRO19622 for rat or human nuclear steroid receptors was evaluated by measuring its ability to compete with specific radioactive ligand binding as described previously (Eckert and Katzenellenbogen, 1982; Inoue et al., 1983; Schilling and Liao, 1984; Sheen et al., 1985; Ross et al., 1991; Clark et al., 1996). Functional interaction of TRO19622 with progesterone receptors (either of the A or the B isoform), the glucocorticoid receptor and the pregnane X receptor was also evaluated in gene reporter assays as described previously (Massaad et al., 1998; Raucy et al., 2002).

In Vitro Binding to Translocator Protein 18 kDa (Peripheral Benzodiazepine Receptor). The affinity of TRO19622 for the translocator protein 18 kDa (TSPO) was evaluated by measuring its ability to compete with [^{3}H]PK11195 binding to either membrane preparations from rat heart (Le Fur et al., 1983) or recombinant mouse TSPO-containing proteoliposomes (Lacapère et al., 2001). In the latter condition, TSPO-containing liposomes (2 μg of protein) were incubated at room temperature for 30 min in the presence of 3 nM [^{3}H]PK11195 (100% initial PK11195 binding; specific activity, 83.5 Ci/mmol) or for 60 min in the presence of 3 nM [^{3}H]cholesterol (100% initial cholesterol binding; specific activity, 60 Ci/mmol). Radioactive ligands were chased by incubation in the presence of increasing concentrations of cold ligands (PK11195, cholesterol, or TRO19622). Vesicle suspensions were filtered on Whatman GF/C filters (Whatman, Maidstone, UK) and washed. Radioactivity was measured by liquid scintillation. Binding data were fitted to a simple sigmoid curve using the following equation $Y = 100 - \text{amp} \times S/(K_d + S)$.

In Vitro Binding to Voltage-Dependent Anion Channel. Photolabeling was performed as described previously (Darbandi-Tonkabon et al., 2003). In brief, rat brain membranes were placed in a quartz cuvette in buffer (50 mM potassium phosphate buffer, pH 7.4, 150 mM NaCl, and 1 mM EDTA) at a concentration of 400 μg of membrane protein/ml and preincubated with either 1 or 3 μM TRO19622, 30 μM 3α5β-TH PROG, or 30 μM 3α5α-TH PROG for 1 h at 4°C in presence of 10 μM GABA. [^{3}H]6-Azi-3α-hydroxy-5β-pregnan-20-one (6-AziP) at 1 μM was then added, and the samples were further preincubated for 20 min at 4°C in the dark. The cuvette was placed in a photoreactor at a distance of 8 cm from the source. The photoreactor uses a 450-W Hanovia medium pressure mercury lamp (Hanovia Ltd., Slough, Berkshire, UK) as the light source. The lamp is cooled by a circulating cold water jacket, and the light is filtered through a 1.5-cm-thick saturated copper sulfate solution. This filter absorbs all light of wavelength <315 nm (Katzenellenbogen et al., 1974). The samples were routinely irradiated for 1 min and continuously cooled to 4°C. Following irradiation the membranes were harvested by centrifugation, solubilized in SDS-sample buffer [125 mM Tris-HCl, pH 6.8, 4% SDS, 0.1 M dithiothreitol, 20% (v/v) glycerol, and 0.004% bromphenol blue], and analyzed by electrophoresis on a 10% SDS-polyacrylamide gel electrophoresis gel. The gels were then sliced, and the radioactivity was measured in each slice. The data were analyzed by integrating the area under the curve of radioactivity peak corresponding to VDAC proteins (35 kDa).

Cerebellar Granule Cell Apoptosis and Quantification of Cytochrome *c*. Primary cultures of rat cerebellar granule cells (CGCs) were prepared from dissociated cerebella of 5-day-old Sprague-Dawley rats as described previously (Drejer et al., 1983). Cells were plated in Dulbecco's modified Eagle's medium supplemented with 10% fetal calf serum, 25 mM KCl, and 0.15 g/l glucose (final concentration 6 g/l) on polyornithine-coated dishes (2.5×10^6 cells/dish). Cytosine arabinoside (10 μM) was added to the culture medium 24 h after plating to prevent proliferation of non-neuronal cells. Apoptosis was induced at 6 days in vitro. Cells were washed and switched to serum-free Dulbecco's modified Eagle's medium containing 5 mM KCl (McGinnis et al., 1999). Mock cells were maintained in the same culture medium. All the compounds used were added to the cell culture medium 6 h before induction of apoptosis. Cells were homogenized 16 h later in 20 mM HEPES, pH 7.4, 10 mM KCl, 1.5 mM $MgCl_2$, 1 mM EDTA, 250 mM sucrose, and 1 mM dithiothreitol, with protease inhibitor cocktail (Roche Diagnostics, Mannheim, Germany). The homogenate was centrifuged at 500*g* for 5 min at 4°C, and the supernatant was centrifuged at 16,000*g* for 30 min. The mitochondrial pellet was washed and centrifuged again at 16,000*g* for 15 min at 4°C. Cytochrome *c* levels in mitochondrial and cytosolic fractions were measured by enzyme-linked immunosorbent assay (Quantikine M; R&D Systems, Minneapolis, MN). Mitochondrial cytochrome *c* was expressed as a percentage of total cytochrome *c*.

Motor Neuron Survival after Axotomy of Facial Nerve in Newborn Rat. Two- to 3-day-old rat pups were anesthetized by hypothermia. The left facial nerve was transected at the stylomastoid foramen. Care was taken to remove a 2-mm segment of the nerve to prevent reinnervation of the distal nerve stump. Animals were treated with test compounds 4 h before surgery and then once a day for 5 days. TRO19622 was given orally, at 10, 30, or 100 mg/kg. The control group received an equivalent amount of vehicle. Animals were sacrificed 7 days after axotomy for the determination of neuronal survival.

Brainstems were removed, dehydrated, and embedded in paraffin. Coronal sections (7 μm in thickness) were taken through the full extent of bilateral facial nuclei, and they were stained with cresyl violet as described previously (Michaelidis et al., 1996). Manual counting was performed on every fifth section. Results were expressed as the percentage of surviving motor neurons compared with the sham-operated contralateral side. Groups included 17 to 20 animals.

Sciatic Nerve Regeneration in Adult Mice. Eight-week-old C57bl/6 RJ mice were anesthetized using 60 mg/kg i.p. ketamine chlorohydrate. To reduce the risk of gender-related differences in response to TRO19622, only female mice were used. The right sciatic nerve was surgically exposed at mid-thigh level, and it was crushed 5 mm proximal to the trifurcation of the sciatic nerve. The nerve was crushed twice for 30 s with hemostatic forceps (width, 1.5 mm; Koenig, Strasbourg, France) with a 90° rotation between each crush. Sciatic nerve degeneration/regeneration was assessed over 6 weeks by measurement of the compound muscular action potential (CMAP) and histological studies of the damaged area of the sciatic nerve. TRO19622 was given subcutaneously at 0.3, 3, and 30 mg/kg. Treatments started the day of the crush injury, and they continued daily for 6 weeks. In total, 15 animals per group were used in the study. Electromyography was performed once a week for 6 weeks using a Neuromatic 2000M electromyograph (Dantec, Les Ulis, France). Mice were anesthetized using 100 mg/kg i.p. ketamine chlorohydrate. CMAP was measured in the gastrocnemius muscle after a single 0.2-ms stimulation of the sciatic nerve at supramaximal intensity (12.8 mA). The amplitude (millivolts) and the latency (milliseconds) of the action potential were measured.

Morphometric analysis of the lesioned nerve was performed at the end of the study. Sciatic nerves were harvested at week 4 and 6 postlesion from five animals per group, and they were processed for Epon embedding. Analysis was performed at the mid-lesion site on 1.5-μm-thick cross sections stained with 1% toluidine blue on the entire surface of the nerve section using semiautomated digital image analysis software (Biocom, Les Ulis, France). Once extraneous objects had been eliminated, the software reported the total number of myelinated fibers. The number of degenerated fibers was then counted manually by an operator blinded in regard to the treatment. Myelinated fibers were scored as degenerated when the myelin buckled and prolapsed within the axoplasm forming onion bulbs. Morphological analysis was performed only on nondegenerated fibers. For each nondegenerated fiber, the axonal and myelin surface areas (square micrometers) were used to calculate the g-ratio (axonal diameter/fiber diameter), indicative of the relative myelin sheath thickness.

ALS Model Transgenic Mice. SOD1^{G93A} transgenic mice, which express the human SOD1 gene containing the G93A mutation [the

B6SJL-TgN(SOD1-G93A)1Gur line; The Jackson Laboratory, Bar Harbor, ME] (Gurney et al., 1994), were maintained as hemizygotes by breeding transgenic males with B6SJLF1/J hybrid females. Transgenic offspring were genotyped for expression of the transgene by polymerase chain reaction assay. Male and female $SOD1^{G93A}$ mice in equal numbers were treated from postnatal day 60 until death by daily subcutaneous injections with either 3 or 30 mg/kg TRO19622 or with the vehicle. Endpoints scored included body weight, motor behavioral testing, electromyographic recordings, and survival. In this study, 11 mice per group were used, although some animals did not recover from anesthesia used to perform electromyography, and they were excluded from survival analysis.

Motor performance was assessed using the grid test. The apparatus consists of a horizontal grid (length, 45 cm; width, 10.5 cm; size of the mesh, 1 × 1 cm) mounted 20 cm above a flat surface support. Mice were lifted by the tail, and they were slowly placed on the edge of the grid and then released. The number of stumbles was counted during walking of a 37-cm distance on the grid. Cut-off value was set as 30 stumbles. In cases where the animal was unable to complete the required 37-cm distance, the test was stopped after 3 min, and the worst score was assigned.

Brain and Plasma Levels of TRO19622. Brain and blood samples were harvested after daily subcutaneous administration of 0.3, 3, and 30 mg/kg TRO19622 to adult mice for a 6-week treatment period. Samples were harvested on weeks 1 and 6, 4 h after dosing, and they were stored at −20°C. Concentrations of TRO19622 were determined by high-performance liquid chromatography with tandem mass spectrometry detection.

Results

Primary Screening Using Purified Motor Neurons. To allow us to perform medium-throughput screening on primary motor neurons, we developed a new instrument, the Flash Cytometer, that allows rapid and fully automated counting of single adherent cells (Supplemental Fig. 1). This fluorescence-based image analyzer was designed to count calcein-stained live neurons or other cells by rapidly capturing fluorescent images encompassing the entire well of 96-well or 384-well culture dishes. Subsequently, dedicated image analysis software distinguished cell bodies from debris or aggregates, and it automatically evaluated the number of live neurons in each well (Valenza et al., 2005; Estévez et al., 2006; Jacquier et al., 2006). This technological breakthrough allowed for screening of approximately 1500 compounds per week, the throughput being limited only by the number of motor neuron cultures that could be prepared. A program of chemical optimization based on the hits coming from a collection of ~40,000 low-molecular-weight compounds culminated in the selection of TRO19622 as one of the compounds with the most potent survival-promoting effects for motor neurons. TRO19622 is a novel cholesterol-like small molecule (399 mol. wt.) (Fig. 1).

Effects of TRO19622 on Motor Neuron Survival and Neurite Outgrowth in Vitro. When purified motor neurons were cultured in the absence of neurotrophic factors for 3 days, the addition of TRO19622 at concentrations ranging from 0.1 to 10 μM led to dose-dependent rescue of motor neurons (Fig. 2). At its maximal tested concentration of 10 μM, TRO19622 maintained survival of 74 ± 10% (n = 8) of the neurons supported by a cocktail of trophic factors (1 ng/ml brain-derived neurotrophic factor, 1 ng/ml glia-derived neurotrophic factor, and 10 ng/ml ciliary neurotrophic factor), defined as 100%. The EC_{50} in this in vitro assay was 3.2 ± 0.2 μM (mean ± S.E.M.; n = 8 wells). TRO19622, like

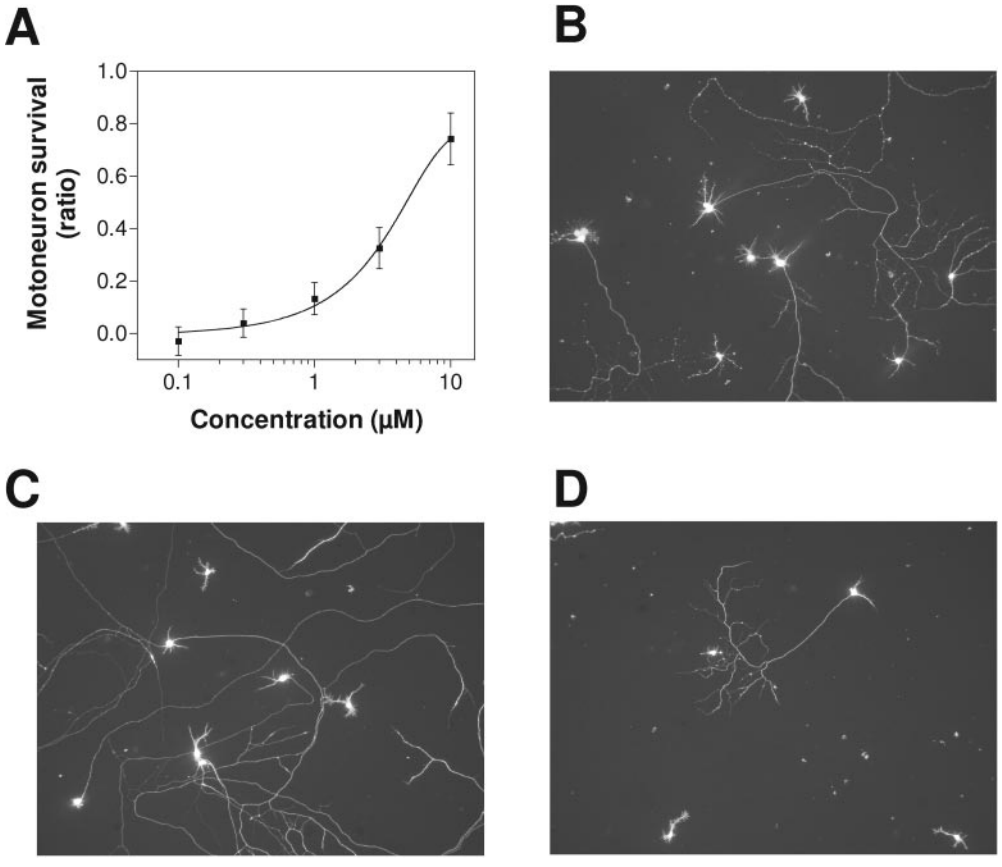

Fig. 2. TRO19622 protects motor neurons from cell death induced by trophic factor deprivation. A, rat embryonic motor neurons were cultured in the absence of trophic factors and with increasing concentrations of TRO19622 (in 0.1% DMSO) in 96-well plates (n = 8 wells/concentration). Motor neuron survival was measured after 3 days in vitro by direct counting of live cells labeled with a fluorescent vital dye, calcein-AM. Survival is expressed as a ratio of surviving cell in each well relative to positive controls treated with a cocktail of neurotrophic factors (defined as 1.0) and negative controls that received DMSO alone (defined as 0.0). Investigation of doses above 10 μM was limited due to poor solubility of TRO19622 in culture medium. Representative micrographs of surviving motor neurons are shown in presence of 5 μM TRO19622 (B), neurotrophic factors (C), and 0.1% DMSO (D).

TABLE 1
Neurite outgrowth quantification after TRO19622 treatment
The effects of low doses of TRO19622 were compared with those of optimal concentrations of neurotrophic factors. Images obtained using the flash cytometer were analyzed automatically using the MetaMorph Neurite Outgrowth Application Module. Values are means ± S.D. (n = 6–8 wells).

Treatment	No. Surviving Cells/Well	Neurite Outgrowth/Cell[a]	Processes/Cell	Branches/Cell
DMSO	137 ± 12	18.5 ± 2.4	1.17 ± 0.09	0.33 ± 0.07
Neurotrophic factors	428 ± 59*	39.4 ± 3.6*	2.18 ± 0.12*	1.20 ± 0.13*
TRO19622, 1 μM	190 ± 10*	28.5 ± 4.5*	1.48 ± 0.11*	0.66 ± 0.25*

* Significantly different ($p < 0.05$) from control DMSO values using the Student's t test.
[a] Arbitrary unit (MetaMorph Neurite Outgrowth Application Module).

other oximes, exists in solution as a mixture of the syn- and antistereoisomers (40:60 ± 10%). Testing of purified syn- and antiforms showed that both were active with no significant difference in potency or efficacy (data not shown). Interestingly, TRO19622 not only preserved motor neuron cell bodies but also promoted neurite outgrowth compared with DMSO-treated motor neurons (Table 1; Supplemental Fig. 1), even at a low dose of 1 μM, which produced only a 38% increase in survival. TRO19622 increased overall neurite outgrowth per cell by 54%. An even more striking effect was observed on the number of axonal branches per cell (increased by 100% compared with DMSO), suggesting that TRO19622 might directly enhance terminal sprouting. Neurite outgrowth values with optimal concentrations of neurotrophic factors were used as a comparison (Table 1). Their effects were stronger, still but this may in part reflect the strong increase (212%) in cell density.

In Vivo Efficacy Studies. In the absence of animal models with proven predictive value for efficacy in sporadic ALS patients, in vivo activity of TRO19622 was evaluated in several animal models of motor neuron degeneration or regeneration. Lesion models were used to probe TRO19622 effects either on motor neuron death (neonatal nerve axotomy) or on axonal degeneration/regeneration (nerve crush) whereas mutant SOD1 mice were used as a model of familial forms of ALS. We used different routes of drug administration depending on the duration of the studies. To avoid the stress of daily oral gavage in long-term studies (nerve crush and $SOD1^{G93A}$ mice), we used the subcutaneous route. In parallel, to demonstrate oral efficacy, we treated rat in the axotomy study per os. Plasma and brain TRO19622 concentrations were determined in control mice having received a daily subcutaneous administration of TRO19622 for a 6-week treatment period (Table 2). Exposure was dose-related, and plasma levels had reached steady state by week 1, and they remained stable over the 6-week treatment period. Brain concentrations were also dose-dependent and relatively stable. Mean brain/plasma ratios ranged from 0.2 to 0.5. At the dose of 3 mg/kg/day s.c., plasma and brain levels were on the order of 0.5 μg/ml and 0.2 μg/g (or 1.25 and 0.5 μM), respectively.

TABLE 2
TRO19622 brain and plasma levels after chronic subcutaneous administration

Weeks of Treatment	Dose	Plasma Levels[a]	Brain Levels	Ratio Brain/Plasma
	mg/kg s.c.	*μg/ml*	*μg/g*	
1	0.3	0.06 ± 0.006	BLQ	
	3	0.55 ± 0.07	0.19 ± 0.02	0.35
	30	5.35 ± 1.19	1.23 ± 0.30	0.23
6	0.3	0.06 ± 0.008	BLQ	
	3	0.47 ± 0.01	0.24 ± 0.04	0.51
	30	5.85 ± 1.06	2.66 ± 0.84	0.45

BLQ, below the limit of quantification.
[a] TRO19622 at 1 μg/ml corresponds to 2.5 μM.

Motor Neuron Survival following Motor Axotomy in Newborn Rats. The ability of TRO19622 to promote motor neuron survival or growth in vivo was evaluated using the established paradigm of facial nerve axotomy in neonatal rats, in which degeneration of facial motor neurons is triggered through loss of trophic support. In vehicle-treated animals, the number of motor neuron cell bodies present 7 days after facial nerve axotomy was only 20 ± 2% (n = 17) compared with the number present on the control contralateral side (Fig. 3). When animals were treated orally for 5 days following the lesion, TRO19622 increased motor neuron cell body survival in a dose-dependent manner with significant rescue at the highest dose of 100 mg/kg (Fig. 3). At this dose, motor neuron survival was 29 ± 2% (n = 18) corresponding to a 42% increase in survival compared with vehicle-treated animals. Similar protection was observed with oral administration of TRO19622 at a single dose of 30 mg/kg when it was dissolved in vegetable oil (31 ± 2%; n = 15; data not shown). This was likely due to better oral bioavailability with this vehicle (data not shown).

Sciatic Nerve Regeneration in Adult Mice. The ability of TRO19622 to promote axonal growth in vitro led us to evaluate its potential for enhancing regeneration of peripheral nerve. Sciatic nerve crush in adult mice resulted in a near complete loss of nerve function as demonstrated by a dramatic loss of CMAP amplitude (up to 80%), along with a marked reduction of motor nerve conduction velocity (CMAP

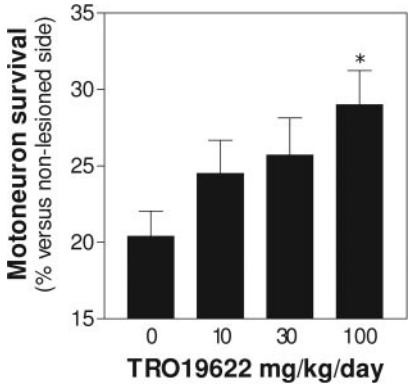

Fig. 3. Neuroprotective effect of TRO19622 on motor neuron survival after neonatal axotomy. Motor neurons were counted in the facial nucleus of 9-day-old rats after right facial nerve transection on postnatal day 2 followed by 5 days of treatment with vehicle or 10, 30, and 100 mg/kg p.o. TRO19622 (n = 17–20). Motor neuron survival in the right facial nucleus (lesioned side) is expressed as a percentage of the number of cells counted in the left nucleus (nonlesioned side). Significantly more motor neurons survived after treatment with TRO19622 at the highest dose. *, $p < 0.05$, Dunnett's multiple comparison test.

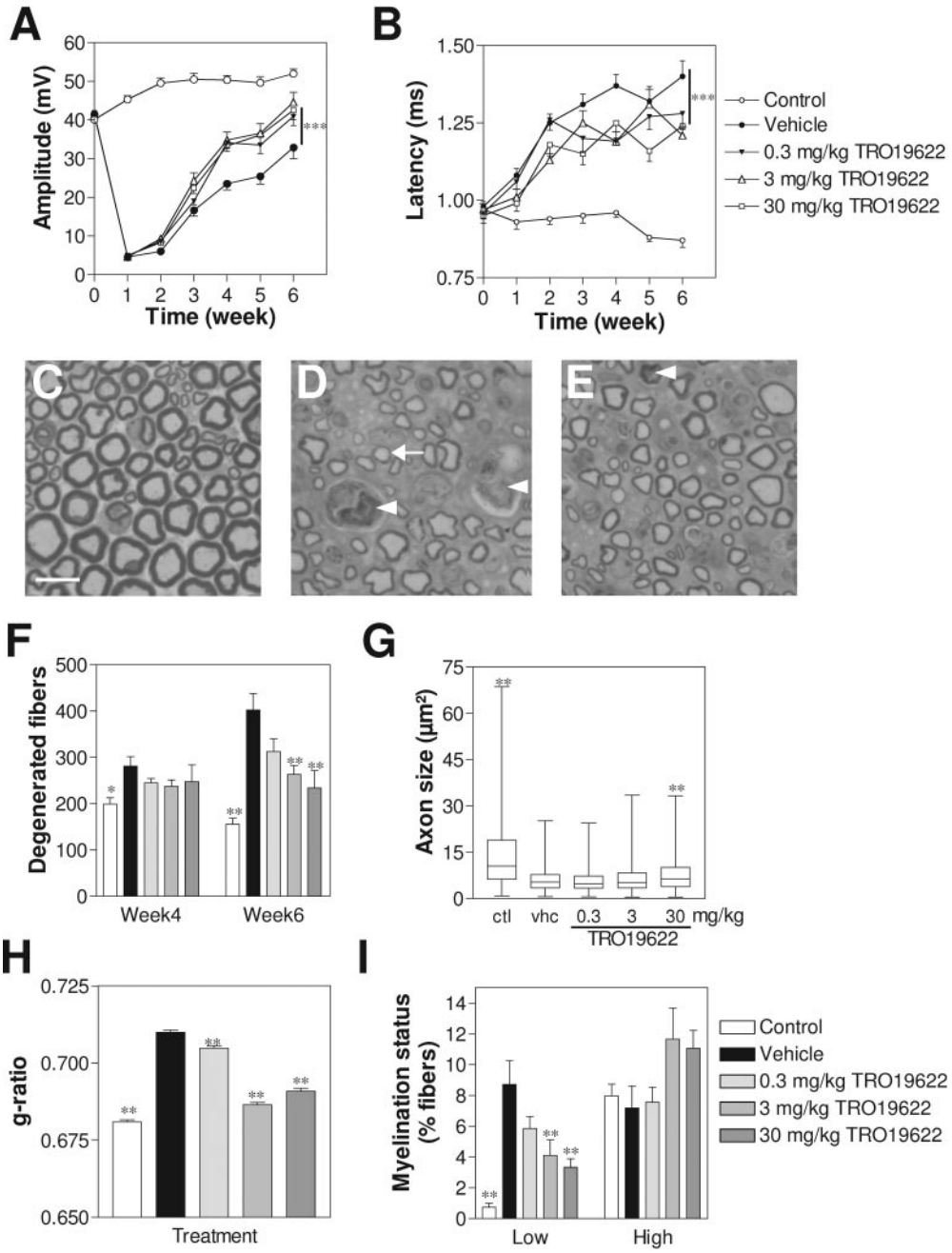

Fig. 4. Effects of TRO19622 on sciatic nerve regeneration. After unilateral lesion of the sciatic nerve, adult mice were treated with vehicle or 0.3, 3, and 30 mg/kg s.c. TRO19622 (n = 15) once a day for 6 weeks. CMAP amplitude (A) and latency (B) were measured every week in lesioned animals and in sham-operated animals (control). C–I, morphometric analysis of the nerve was performed at week 4 and 6 postlesioning in the mid-lesion site. Representative histological micrographs of sciatic nerve tissue of control group (C), vehicle-treated (D), and 30 mg/kg TRO19622-treated (E) groups at week 6 are shown. The density and size of the myelinated fibers after the sciatic nerve crush remain lower than those in the normal mice. In mice treated with TRO19622, there were a higher number of regenerated fibers and a more mature appearance than in vehicle-treated mice as observed by the decrease number of poorly myelinated fibers (white arrow). Number of degenerated fibers as indicated by arrowhead was also decreased after TRO19622 treatment. Scale bar, 15 μm. F, absolute numbers of degenerated fibers per nerve section are shown at week 4 and week 6 (mean ± S.E.M.; n = 5 animals). G, axonal surface area of nondegenerated myelinated axons was measured 4-weeks postlesion as a function of treatment. Boxes comprise the median and the 25 and 75 percentiles, and horizontal lines denote the highest and lowest values. H, nerve crush led to an increase in g-ratio of nondegenerated fibers, reflecting relative reduction in myelination. This was partially corrected by all doses of TRO19622. I, fibers having a g-ratio ≥ 0.8 were considered as poorly myelinated fibers (low), whereas fibers having g-ratio ≤ 0.6 were considered as highly myelinated fibers (high). Treatment with TRO19622 was strongly protective against the crush-induced increase in numbers of poorly myelinated fibers. Means ± S.E.M., n = 5 animals. *, $p < 0.05$; **, $p < 0.01$, significantly different compared with crush/vehicle group, Dunnett's multiple comparison test.

latency) during the first 2 weeks following the lesion (Fig. 4, A and B). This loss of function was followed at 4 and 6 weeks by an increase in the proportion of degenerated fibers and an overall shrinkage of axonal diameter (Fig. 4, D, F, and G). Spontaneous recovery occurred from week 2 onward as demonstrated by improvement in CMAP amplitude.

Treatment with TRO19622 (0.3, 3, or 30 mg/kg s.c.) led to a dose-dependent acceleration in the regeneration process beginning at week 2 after injury, as indicated by improvements in neuromuscular function (CMAP measurements), reaching significance for all doses by week 4 (Fig. 4A). By week 6, TRO19622-treated mice demonstrated up to 80% recovery of the CMAP level of sham-operated mice (control), whereas recovery was only 60% for vehicle-treated mice. At the highest doses (3 and 30 mg/kg), reductions in the increase of CMAP latency were observed compared with the vehicle-treated group. The differences were apparent 2 weeks after the lesion, reaching 15% reduction by week 6 compared with vehicle-treated animals (Fig. 4B).

To determine whether these electromyographic improvements were correlated with decreased nerve degeneration and/or improved nerve regeneration, a morphometric analysis was performed on nerve sections in the midlesion region 4 and 6 weeks postlesion. By 6 weeks, the number of degenerated fibers was significantly reduced using doses of 3 and 30 mg/kg TRO19622: a 69% reduction relative to control was observed for the 30-mg/kg group (Fig. 4F).

Morphometric analysis of nondegenerated myelinated fibers was performed at week 4 (Fig. 4, G–I) by measuring axonal and myelin surface areas independently. Lesioned nerves from vehicle-treated animals showed an overall reduction in axonal size (both median size and maximum size)

compared with controls (Fig. 4G). Treatment with TRO19622 increased axonal cross-sectional area, reaching statistical significance at the highest dose (mean axonal size ± S.E.M.; 7.6 ± 0.1 μm^2 in the TRO19622 30-mg/kg group, $p < 0.05$ versus 6.0 ± 0.1 μm^2 in the vehicle group; the uncrushed control group measured 14.0 ± 0.2 μm^2). As shown in Fig. 4H, sciatic nerve crush induced a significant increase in the g-ratio, an indicator of relative loss of myelin thickness (see *Materials and Methods*). Importantly, at 4 weeks TRO19622 treatment at all doses induced a significant reduction in g-ratio value with 80% correction at the dose of 3 mg/kg. TRO19622-treatment also induced a dose-dependent reduction in "poorly" myelinated fibers (g-ratio ≥ 0.8), and a smaller increase in the proportion of "highly" myelinated fibers (g-ratio ≤ 0.6) at the doses of 3 or 30 mg/kg, although the latter difference did not reach statistical significance ($p = 0.077$). Based on both electromyographic and histological results, the dose of 3 mg/kg/day was determined as the minimal effective dose for further studies in transgenic models.

ALS Model Transgenic Mice. Transgenic mice overexpressing the G93A mutated form of the human SOD1 gene are a commonly used model for familial ALS (Gurney et al., 1994). As already reported by others, $SOD1^{G93A}$ mice displayed a progressive decrease in body weight from week 15 onward, along with a decline in grid test performance that is considered indicative of a deficit in motor coordination (Fig. 5).

Treatment of $SOD1^{G93A}$ mice with TRO19622 delayed the onset of many disease signs. At 3 mg/kg/day, we observed a 15-day delay in the onset of the decline of body weight (two-way ANOVA, $p < 0.01$; Fig. 5A). A significant delay of approximately 11 days in the decline of grid performance was observed at both 3- and 30-mg/kg doses (two-way ANOVA from week 14 to 21, $p < 0.01$; Fig. 5B). Finally, treatment with TRO19622 also resulted in a significant increase in life span (Fig. 5C). TRO19622-treated $SOD1^{G93A}$ mice lived 10% longer (138 ± 4 days, $n = 7$ and 135 ± 3 days, $n = 7$, for doses of 3 and 30 mg/kg/day, respectively) than did vehicle-treated controls (125 ± 3 days, $n = 9$). Because the delay in onset was similar in magnitude to the prolongation of life span, we concluded that the major beneficial effect of TRO19622 was on disease onset rather than progression.

Binding Studies to Identify Potential Targets. To identify its potential molecular targets and mechanism of action, TRO19622 was screened at concentrations up to 50 μM in buffered solutions containing 0.2% bovine serum albumin on a large panel of enzymes, receptors, channels, and transporters (Diversity Profile; Cerep). Of the 80 targets screened, only two targets showed a significant displacement of control binding: the progesterone receptor and TSPO, previously named peripheral benzodiazepine receptor (Papadopoulos et al., 2006).

To follow-up on the binding to the progesterone receptor, more detailed studies of interaction with classical nuclear steroid receptors were performed. TRO19622 at 50 μM displaced radioligand binding to the progesterone receptor by only 56%, whereas displacement of less than 20% was observed at lower concentrations (Table 3). A slight interaction was observed with vitamin D_3 although it was judged of low significance in the absence of a dose-effect relationship. No major displacement was observed on other nuclear steroid receptors. To further evaluate the potential agonist or antag-

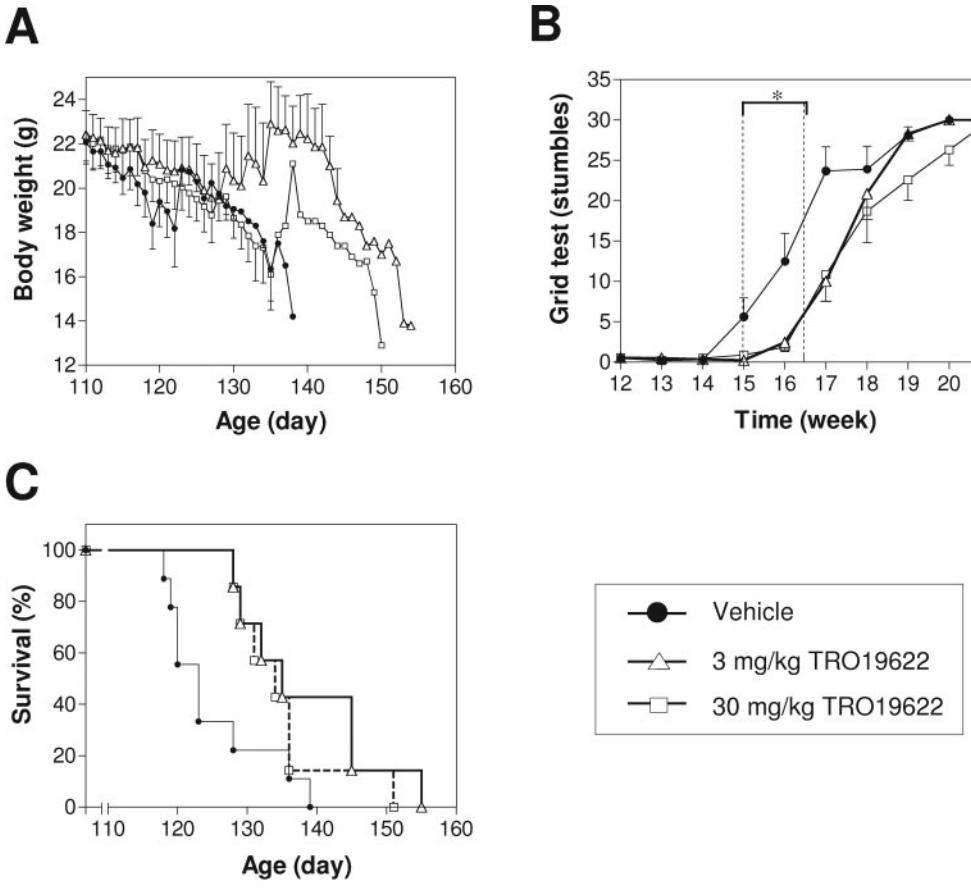

Fig. 5. Beneficial effects of TRO19622 treatment on disease onset and survival of $SOD1^{G93A}$ mice. Effects of TRO19622 treatment on body weight during disease progression (A), motor performance measured in the grid test (B), and life span of $SOD1^{G93A}$ mice (C). There was no negative impact of TRO19622 on weight gain and even a possible beneficial effect on body weight at the lower dose ($n = 11$ mice/group). Both doses of TRO19622, 3 and 30 mg/kg/day, delayed the onset of the clinical disease as measured by loss in motor function ($n = 11$ mice/group), and they significantly prolonged survival by approximately 10% ($n = 7$ mice in TRO19622-treated groups and $n = 9$ mice in the vehicle-treated group). *, $p < 0.05$, two-way ANOVA test compared with vehicle-treated animals.

TABLE 3
TRO19622 binding to nuclear steroid receptors
Inhibition of binding of specific ligands to nuclear steroid receptors by TRO19622 is expressed as a percentage of the control values (means of duplicate values).

Target	Ligand, Concentration	[TRO19622]	Inhibition of Control-Specific Binding
		μM	%
Glucocorticoid (h) (glucocorticoid receptor)	[^{3}H]Triamcinolone, 1.5 nM	50	17
Estrogen (h) (estrogen receptor)	[^{3}H]Estradiol, 1 nM	50	28
Progesterone (h) (PR)	[^{3}H]R-5020, 2 nM	0.3	14
		3	4
		30	19
		50	56
Androgen (androgen receptor)	[^{3}H]Mibolerone, 1 nM	50	−8
Vitamin D_3 (h)	[^{3}H]1α,25-(OH_2)D_3, 0.3 nM	0.3	5
		3	7
		30	6
		50	43
Thyroid hormone	[^{125}I]Triiodothyronine, 0.1 nM	50	−7

onist activity of TRO19622 at progesterone receptors, functional studies were performed using a progesterone gene-reporter assay in MSC80 cells (Table 4). TRO19622 at concentration up to 10 μM did not activate the endogenous glucocorticoid receptor. When cells were cotransfected with progesterone receptor-expressing plasmids, TRO19622 at concentrations up to 10 μM neither activated progesterone receptors (either the A or B isoform, PRA or PRB) on its own nor prevented their activation using concentrations of progesterone as low as 10 nM (Table 4). Likewise, TRO19622 neither activated the orphan pregnane X receptor nor prevented its activation by rifampicin in a gene-reporter assay (Table 4). Therefore, TRO19622 does not interact functionally with classical nuclear steroid receptors.

TRO19622 Targets Components of the Mitochondrial Permeability Transition Pore. TRO19622 displacement of 0.2 nM [^{3}H]PK11195 binding to TSPO in rat heart membranes displayed an IC_{50} value of 30 to 50 μM (48 ± 2% inhibition of specific binding at 30 μM and 62 ± 11% at 50 μM). TRO19622 was therefore studied for its ability to displace the binding of PK11195 to purified recombinant mouse TSPO reconstituted into proteoliposomes (Lacapère et al., 2001). Surprisingly, only a slight decrease in binding of radioactive PK11195 was observed, and this was independent of TRO19622 concentration (Fig. 6A). An alternative possibility came from the report that TSPO is a mitochondrial cholesterol transporter (Lacapère and Papadopoulos, 2003; Jamin et al., 2005). Because TRO19622 has a cholesterol-like structure, its ability to displace the binding of cholesterol to TSPO was also tested. TRO19622 significantly displaced [^{3}H]cholesterol binding to recombinant TSPO with a K_i of 100 nM (Fig. 6B), indicating that TRO19622 interacts with TSPO at the cholesterol site rather than at the PK11195 binding site.

One of the roles of TSPO is as part of the mitochondrial permeability transition pore complex (mPTP) where it is closely associated with VDAC in the outer mitochondrial membrane. Interestingly, specific binding of neuroactive steroids to VDAC has been demonstrated using [^{3}H]6-AziP, a photoaffinity analog of pregnanolone (3α5β-TH PROG) (Darbandi-Tonkabon et al., 2003). We therefore investigated the interaction of TRO19622 with the neurosteroid site on VDAC by measuring its ability to modulate covalent labeling of VDAC in rat brain membranes by [^{3}H]6-AziP. Low concentrations of TRO19622 (1–3 μM) reduced photolabeling of VDAC by 6-AziP in a dose-dependent manner, suggesting a competitive interaction between 6-AziP and TRO19622. TRO19622 at 3 μM reduced photolabeling by 55 ± 10% (Fig. 7). A similar degree of inhibition was observed with a 5β-reduced steroid (pregnanolone, 3α5β-TH PROG) at 30 μM (45 ± 1%). In contrast, a 5α-reduced steroid (allopregnanolone, 3α5α-TH PROG) did not compete with the photolabeling of VDAC by 6-AziP (10 ± 2% inhibition), suggesting that this binding site is stereoselective.

TABLE 4
TRO19622 did not functionally interact with steroid nuclear receptors in gene reporter assays
Gene reporter cell lines (MSC80 for glucocorticoid and progesterone receptor activation; C1F1 for pregnane X receptor induction) were exposed to the compounds for 48 h, and reporter activities were assessed. Values are expressed as means of the fold increase in activity above that in DMSO-treated cells ± S.D. (n = 3).

Steroid Nuclear Receptor	Compound	Fold Induction Relative to DMSO
Glucocorticoid receptor	TRO19622, 3 μM	1.05 ± 0.05
	TRO19622, 10 μM	1.36 ± 0.08
PRA	TRO19622, 3 μM	0.86 ± 0.03
	TRO19622, 10 μM	0.87 ± 0.05
	Progesterone, 10 nM	2.36 ± 0.42*
	Progesterone, 10 nM + TRO19622, 10 μM	2.09 ± 0.24*
PRB	TRO19622, 3 μM	1.11 ± 0.04
	TRO19622, 10 μM	0.97 ± 0.12
	Progesterone, 10 nM	2.23 ± 0.19*
	Progesterone, 10 nM + TRO19622, 10 μM	1.92 ± 0.23*
Pregnane X receptor	TRO19622, 3 μM	0.65 ± 0.09*
	TRO19622, 10 μM	0.96 ± 0.12
	Rifampicin, 10 μM	3.50 ± 0.32*
	Rifampicin, 10 μM + TRO19622, 3 μM	2.90 ± 0.36*

* Significantly different ($p < 0.05$) than basal values in the control DMSO samples using ANOVA with a Dunnett's post test.

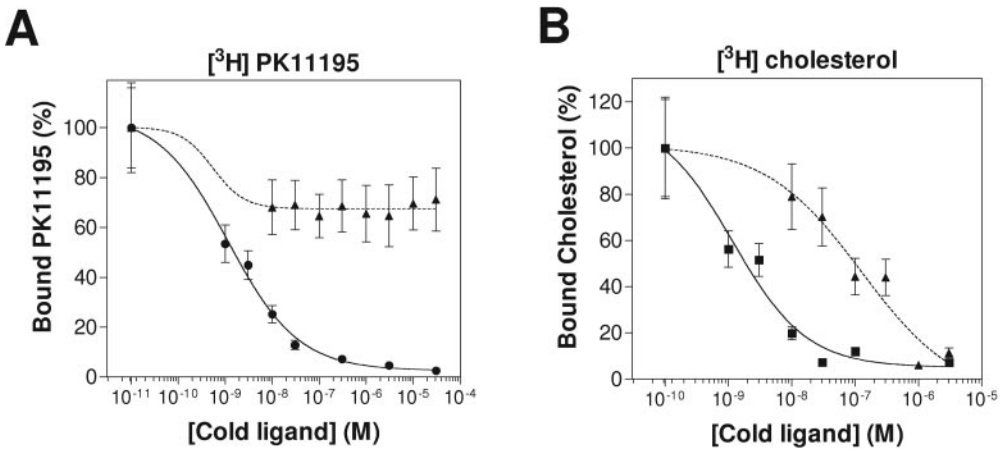

Fig. 6. TRO19622 binding to recombinant TSPO. Interaction of TRO19622 with recombinant TSPO-reconstituted in liposomes was performed as described under *Materials and Methods* using [^{3}H]PK11195 (A) or [^{3}H]cholesterol (B). Displacement of specific TSPO radioligands binding by increasing concentration of cold TRO19622 (triangles), PK11195 (circles), or cholesterol (squares) is shown. Data fitting for PK11195 and cholesterol gives IC_{50} values of 2 nM for both compounds. Results are representative of four to five independent experiments performed in triplicate (mean ± S.E.M.).

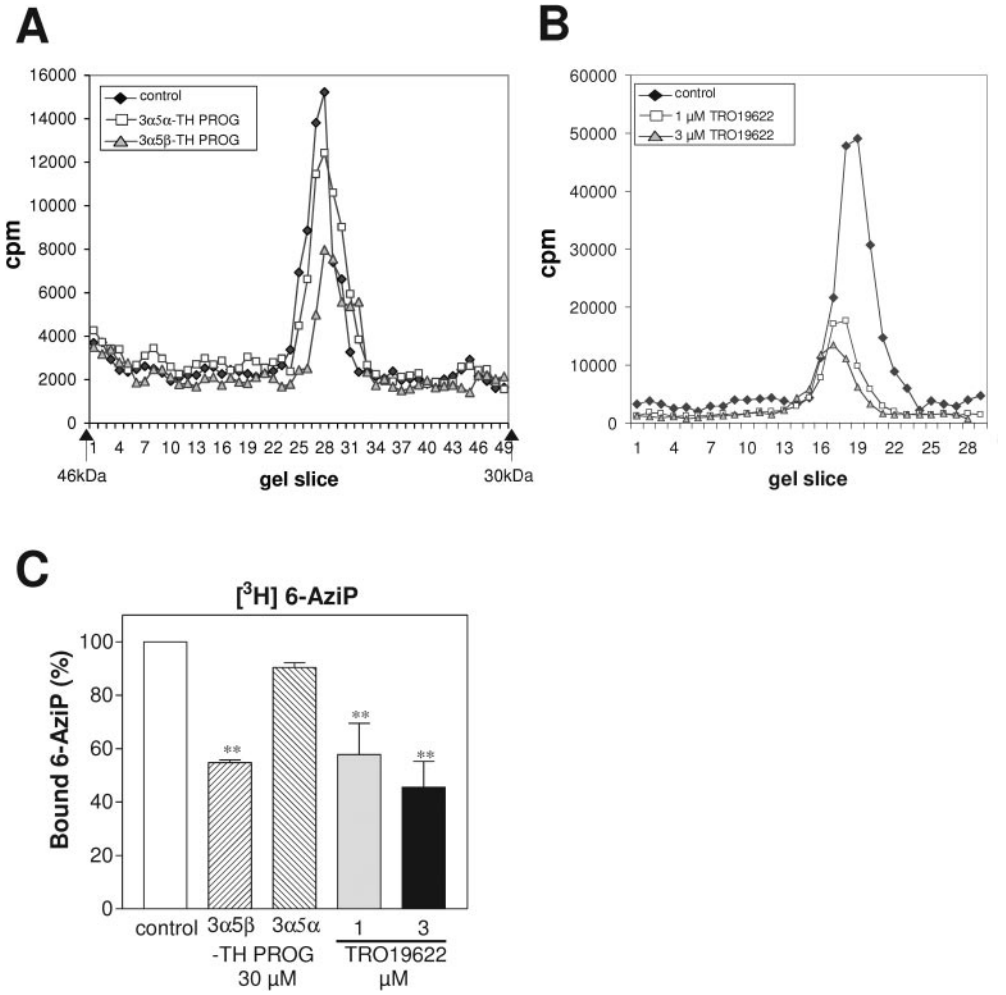

Fig. 7. TRO19622 binding to VDAC. Rat brain membranes were incubated with 1 μM [^{3}H]6-AziP in the presence of 1 and 3 μM TRO19622, 30 μM 3α5β-TH PROG, or 30 μM 3α5α-TH PROG, and photolabeling was performed by UV irradiation for 1 min. Proteins were separated by SDS-polyacrylamide gel electrophoresis, and radioactivity in slicing was determined by scintillation counting. Representative experiments are shown in A and B. C, specific labeling of VDAC proteins (35 kDa) was measured, and the area under of the curve was expressed as percentage of control labeling. Mean ± S.E.M., $n = 2$ to 3 individual experiments; **, $p < 0.01$, significantly different compared with control, Dunnett's multiple comparison test.

These findings raised the possibility that the neuroprotective effects of TRO19622 might be explained by inhibition of mPTP opening, for which a role in programmed cell death has frequently been proposed. To investigate functional effects of TRO19622 binding at the mitochondrial level, we tested its ability to modulate cytochrome *c* release. We used the death of cerebellar granule cells triggered by low potassium as a model because the role of mPTP opening in apoptosis is well documented in this system (Precht et al., 2005). Neuronal apoptosis was triggered in CGCs by transferring the cells into low-potassium culture medium. Sixteen hours after induction of apoptosis, cytochrome *c* was quantified by enzyme-linked immunosorbent assay in mitochondrial and cytoplasmic fractions. The fraction of cytochrome *c* in mitochondria decreased from 34% of total cytochrome *c* in mock controls to 20% following induction of apoptosis; total cytochrome *c* levels were unchanged (Table 5). Pretreatment with TRO19622 at 3 μM led to retention of 30% of total cytochrome *c* in mitochondria. Similar inhibition of cytochrome

TABLE 5
TRO19622 prevents cytochrome *c* release from mitochondria in CGCs
Mitochondrial cytochrome *c* levels are expressed as a percentage of total cytochrome *c*. Three experiments gave similar results: a representative example is shown.

Treatment	Cytochrome *c*			Mitochondrial Cytochrome *c*
	Mitochondria	Cytosol	Total	
	ng			%
Mock	17.2	33.8	51	33.7*
Low K^+ apoptosis	10.8	44	54.8	19.7
Low K^+ + TRO19622, 3 μM	15.6	37.2	52.8	29.6*
Low K^+ + CsA, 10 μM	16.6	37.3	53.9	30.8*

* Significantly different ($p < 0.05$) from percentage values in the control low potassium-induced apoptosis samples using the Student's *t* test.

c release was observed after pretreatment with 10 μM CsA, a known inhibitor of mPTP opening.

Discussion

Using a phenotypic cell-based screening approach, we report the discovery of TRO19622, a low-molecular-weight compound that potently enhances motor neuron survival and growth in culture. TRO19622 is also active in vivo in three animal models of motor neuron degeneration, demonstrating the predictive value of the cell-based assay. The finding that TRO19622 interacts with protein components of the mitochondrial permeability transition pore defines these as potential new therapeutic targets for the diverse traumatic and genetic lesions of the motor system that involve mitochondrial dysfunction.

TRO19622 as Drug Candidate. In vitro, TRO19622 was nearly as effective as a cocktail of three neurotrophic factors at maintaining motor neuron survival, and it promoted neurite outgrowth and branching in the same cells. In vivo TRO19622 rescued motor neuron cell bodies from axotomy-induced cell death. TRO19622 also accelerated spontaneous nerve recovery after nerve crush as measured by enhanced recovery of CMAP amplitude and latency, and earlier functional recovery (data not shown). TRO19622 most likely both slows degeneration and accelerates regeneration of nerve fibers. Numbers of degenerated fibers were significantly reduced by TRO19622 treatment, whereas axonal sizes of lesioned nerves, a marker of axonal regeneration (Funakoshi et al., 1998), were increased. Unexpectedly, TRO19622 seemed also to affect other functionally relevant processes. By week 4 of drug treatment, muscle electromyographic parameters were improved in the absence of changes in the density of degenerating fibers, suggesting that TRO19622 may have beneficial effects on neuromuscular junction function. Moreover, TRO19622 treatment led to an increase in the proportion of "highly" myelinated fibers, suggesting that part of the beneficial effect of TRO19622 may be due to effects on glia.

Enhancing axonal sprouting and regeneration would be expected to be beneficial in ALS, in which axonal dying back plays an early role (Gordon et al., 2004; Precht et al., 2005; Pun et al., 2006). Indeed, in $SOD1^{G93A}$ transgenic mice, the 10% increase in the survival time provided by TRO19622 seemed mostly to be explained by the delay in onset of motor dysfunction and weight loss. Importantly, even daily administration for more than 2 months was very well tolerated, without any toxicity or adverse side effects.

TRO19622 Mechanism of Action and Target. The chemical structure of TRO19622 led us to explore potential targets for steroids and neurosteroids. We first demonstrated that TRO19622 does not interact functionally with classical nuclear steroid receptor. However, binding sites for TRO19622 were identified on two proteins of the outer mitochondrial membrane, TSPO (previously named peripheral benzodiazepine receptor) and VDAC.

TSPO is a mitochondrial cholesterol, porphyrin, and protein transporter. Other TSPO ligands have been reported to have beneficial effects on motor nerve regeneration (Ferzaz et al., 2002), possibly by inducing increased synthesis of neurosteroids. TRO19622 interacts with the cholesterol binding site on TSPO with a K_i value of 100 nM. However, given that the K_d value for cholesterol itself is below 10 nM (Lacapère et al., 2001; Jamin et al., 2005) and that the plasma concentration of cholesterol is ~1000-fold higher than that required for efficacy of TRO19622, it is unlikely that TRO19622 binding to this site has any impact on cholesterol metabolism or steroidogenesis. However, it is conceivable that this site may permit uptake of TRO19622 into mitochondria, and its concentration in steroidogenic tissues. Indeed, although preclinical safety and toxicology studies showed no effect on steroid-sensitive organs or steroid hormone levels, a mass balance study of [^{14}C]TRO19622 in rats showed the highest accumulation in adrenal cortex (T. Bordet and R. M. Pruss, unpublished data).

Investigation of other nonconventional steroid binding sites led us to explore an interaction between TRO19622 and VDAC, a specific target for certain neuroactive steroids (Darbandi-Tonkabon et al., 2003). We could demonstrate direct interactions between TRO19622 and VDAC in rat brain membranes. These membranes contain both VDAC1 and VDAC2 (Darbandi-Tonkabon et al., 2004), and it is probable that TRO19622 interacts with both proteins, although this is still under investigation. Interestingly, TRO19622 binding to VDAC seems to be more potent than that of the natural neurosteroid 3α,5β-TH PROG. The specificity and potential biological significance of this steroid binding site on VDAC is emphasized by the exquisite stereoselectivity of this site for 5β- over 5α-reduced steroids. This binding site seems to be able to accommodate the unsaturated A-ring of TRO19622. Interestingly, during the course of these studies, it was observed that TRO19622 interactions with VDAC were increased in the presence of GABA (data not shown). Although the mechanism by which GABA enhances TRO19622 binding remains to be explored, it is interesting that VDAC1 is known to associate with $GABA_A$ receptors (Bureau et al., 1992). Because $GABA_A$ receptors are mainly concentrated at synapses, TRO19622 may preferentially target mitochondria at synapses.

VDAC, also called porin, is the major transport protein in

the outer membrane of the mitochondria (for recent review, see Shoshan-Barmatz et al., 2006). In close association with proteins at the inner membrane, such as the adenine nucleotide transporter ANT1 and cyclophilin D, VDAC is thought to contribute to the mPTP complex, which transports anions, cations, ATP, calcium, and metabolites between mitochondria and cytosol, and it has been proposed to enable the release of apoptogenic proteins by mitochondria during cell death. However, study of knockout mice recently demonstrated that VDAC is dispensable both for pore activity and cell death (Baines et al., 2007). We speculate that the neuroprotective effects of TRO19622 might, at least in part, be due to its binding to VDAC. Here, we showed that TRO19622 reduces cytochrome *c* release in CGCs when cultured in low potassium. This is consistent with direct inhibition of mPTP opening, but it could also be explained by indirect effects on mitochondrial function.

Mitochondria as a Target in ALS. It is striking that a compound identified through its neuroprotective action should show specific binding to two mitochondrial proteins. Although it may also act through other mechanisms, this site of action of TRO19622 is relevant because mitochondrial dysfunction has been largely implicated in the pathophysiology of ALS (for review, see Manfredi and Xu, 2005). Abnormal mitochondrial morphology, including swelling and vacuolization, have been described both in skeletal muscles and in the anterior horn of ALS patients (Afifi et al., 1966; Sasaki and Iwata, 1996; Echaniz-Laguna et al., 2006) and in mutant $SOD1^{G93A}$ mice before symptom onset. Moreover, mutant forms of SOD1, a normally cytoplasmic enzyme, show increased association with (or even incorporation into) the mitochondrial membrane in affected, but not unaffected, tissues (Liu et al., 2004; Bergemalm et al., 2006; Deng et al., 2006). Mitochondria play a pivotal role in cell death, and they are also important regulators of intracellular calcium homeostasis and ATP production. Recently, Gould et al. (2006) found that mutant SOD1 accumulated in nerve terminals and that it was associated with mitochondrial vacuolization as early as 25 days of age, corresponding to the onset of neuromuscular denervation but before motor neuron cell death in $SOD1^{G93A}$ mice. Crossing $SOD1^{G93A}$ mice with Bax knockout mice increased life span by approximately 15%, correlated with a delay in mitochondrial vacuolization and neuromuscular denervation, but dissociated from motor neuron cell death. Bax deletion may therefore delay death of $SOD1^{G93A}$ mice not through prevention of motor neuron cell death but by maintaining denervation-induced sprouting either through delay of mitochondrial dysfunction and/or maintenance of axoplasmic trafficking (Gould et al., 2006). Although this would be an attractive explanation for the delay in onset provided by TRO19622, our data do not provide definitive proof for such a model.

In conclusion, TRO19622, identified for its survival-promoting properties for motor neurons in culture has been shown to have both neuroprotective and neuroregenerative properties in a number of in vivo models of neurodegeneration. Based on these preclinical indicators of efficacy, we think that TRO19622 has therapeutic potential for ALS and other motor neuron diseases such as spinal muscular atrophy. TRO19622 may also have potential in other neurodegenerative diseases or indications where trophic factor deprivation and/or mitochondrial dysfunction have been implicated.

Acknowledgments

We thank Drs. Toni Williamson and Pascal Villa for initiating the project and Antoine Béret for continuous encouragement. We thank the Trophos screening team for expert technical assistance and Neurofit (Strasbourg, France) for the contribution to in vivo testing. We are grateful to Drs. Catherine Rousselot and François Bellamy for invaluable support in preclinical development.

References

Afifi AK, Aleu FP, Goodgold J, and MacKay B (1966) Ultrastructure of atrophic muscle in amyotrophic lateral sclerosis. *Neurology* **16:**475–481.

Apfel SC (2001) Neurotrophic factor therapy–prospects and problems. *Clin Chem Lab Med* **39:**351–355.

Baines CP, Kaiser RA, Sheiko T, Craigen WJ, and Molkentin JD (2007) Voltage-dependent anion channels are dispensable for mitochondrial-dependent cell death. *Nat Cell Biol* **9:**550–555.

Bendotti C and Carri MT (2004) Lessons from models of SOD1-linked familial ALS. *Trends Mol Med* **10:**393–400.

Bensimon G, Lacomblez L, and Meininger V (1994) A controlled trial of riluzole in amyotrophic lateral sclerosis. *N Engl J Med* **330:**585–591.

Bergemalm D, Jonsson PA, Graffmo KS, Andersen PM, Brannstrom T, Rehnmark A, and Marklund SL (2006) Overloading of stable and exclusion of unstable human superoxide dismutase-1 variants in mitochondria of murine amyotrophic lateral sclerosis models. *J Neurosci* **26:**4147–4154.

Bordet T, Lesbordes JC, Rouhani S, Castelnau-Ptakhine L, Schmalbruch H, Haase G, and Kahn A (2001) Protective effects of cardiotrophin-1 adenoviral gene transfer on neuromuscular degeneration in transgenic ALS mice. *Hum Mol Genet* **10:**1925–1933.

Bruijn LI, Miller TM, and Cleveland DW (2004) Unraveling the mechanisms involved in motor neuron degeneration in ALS. *Annu Rev Neurosci* **27:**723–749.

Bureau MH, Khrestchatisky M, Heeren MA, Zambrowicz EB, Kim H, Grisar TM, Colombini M, Tobin AJ, and Olsen RW (1992) Isolation and cloning of a voltage-dependent anion channel-like Mr 36,000 polypeptide from mammalian brain. *J Biol Chem* **267:**8679–8684.

Clark AF, Lane D, Wilson K, Miggans ST, and McCartney MD (1996) Inhibition of dexamethasone-induced cytoskeletal changes in cultured human trabecular meshwork cells by tetrahydrocortisol. *Invest Ophthalmol Vis Sci* **37:**805–813.

Darbandi-Tonkabon R, Hastings WR, Zeng CM, Akk G, Manion BD, Bracamontes JR, Steinbach JH, Mennerick SJ, Covey DF, and Evers AS (2003) Photoaffinity labeling with a neuroactive steroid analogue. 6-Azi-pregnanolone labels voltage-dependent anion channel-1 in rat brain. *J Biol Chem* **278:**13196–13206.

Darbandi-Tonkabon R, Manion BD, Hastings WR, Craigen WJ, Akk G, Bracamontes JR, He Y, Sheiko TV, Steinbach JH, Mennerick SJ, et al. (2004) Neuroactive steroid interactions with voltage-dependent anion channels: lack of relationship to $GABA_A$ receptor modulation and anesthesia. *J Pharmacol Exp Ther* **308:**502–511.

del Aguila MA, Longstreth WT Jr., McGuire V, Koepsell TD, and van Belle G (2003) Prognosis in amyotrophic lateral sclerosis: a population-based study. *Neurology* **60:**813–819.

Deng HX, Shi Y, Furukawa Y, Zhai H, Fu R, Liu E, Gorrie GH, Khan MS, Hung WY, Bigio EH, et al. (2006) Conversion to the amyotrophic lateral sclerosis phenotype is associated with intermolecular linked insoluble aggregates of SOD1 in mitochondria. *Proc Natl Acad Sci U S A* **103:**7142–7147.

Drejer J, Larsson OM, and Schousboe A (1983) Characterization of uptake and release processes for D- and L-aspartate in primary cultures of astrocytes and cerebellar granule cells. *Neurochem Res* **8:**231–243.

Echaniz-Laguna A, Zoll J, Ponsot E, N'Guessan B, Tranchant C, Loeffler JP, and Lampert E (2006) Muscular mitochondrial function in amyotrophic lateral sclerosis is progressively altered as the disease develops: a temporal study in man. *Exp Neurol* **198:**25–30.

Eckert RL and Katzenellenbogen BS (1982) Effects of estrogens and antiestrogens on estrogen receptor dynamics and the induction of progesterone receptor in MCF-7 human breast cancer cells. *Cancer Res* **42:**139–144.

Estévez AG, Sahawneh MA, Lange PS, Bae N, Egea M, and Ratan RR (2006) Arginase 1 regulation of nitric oxide production is key to survival of trophic factor-deprived motor neurons. *J Neurosci* **26:**8512–8516.

Ferzaz B, Brault E, Bourliaud G, Robert JP, Poughon G, Claustre Y, Marguet F, Liere P, Schumacher M, Nowicki JP, et al. (2002) SSR180575 (7-chloro-*N*,*N*,5-trimethyl-4-oxo-3-phenyl-3,5-dihydro-4*H*-pyridazino[4,5-*b*]indole-1-acetamide), a peripheral benzodiazepine receptor ligand, promotes neuronal survival and repair. *J Pharmacol Exp Ther* **301:**1067–1078.

Friedman B, Kleinfeld D, Ip NY, Verge VMK, Moulton R, Boland P, Zlotchenko E, Lindsay RM, and Liu LM (1995) BDNF and NT-4/5 exert neurotrophic influences on injured adult spinal motor neurons. *J Neurosci* **15:**1044–1056.

Funakoshi H, Risling M, Carlstedt T, Lendahl U, Timmusk T, Metsis M, Yamamoto Y, and Ibanez CF (1998) Targeted expression of a multifunctional chimeric neurotrophin in the lesioned sciatic nerve accelerates regeneration of sensory and motor axons. *Proc Natl Acad Sci U S A* **95:**5269–5274.

Gordon T, Hegedus J, and Tam SL (2004) Adaptive and maladaptive motor axonal sprouting in aging and motoneuron disease. *Neurol Res* **26:**174–185.

Gould TW, Buss RR, Vinsant S, Prevette D, Sun W, Knudson CM, Milligan CE, and Oppenheim RW (2006) Complete dissociation of motor neuron death from motor dysfunction by Bax deletion in a mouse model of ALS. *J Neurosci* **26:**8774–8786.

Gurney ME, Pu H, Chiu AY, Dal Canto MC, Polchow CY, Alexander DD, Caliendo J,

Hentati A, Kwon YW, Deng HX, et al. (1994) Motor neuron degeneration in mice that express a human Cu,Zn superoxide dismutase mutation. *Science* **264:**1772–1775.
Haase G, Pettmann B, Bordet T, Villa P, Vigne E, Schmalbruch H, and Kahn A (1999) Therapeutic benefit of ciliary neurotrophic factor in progressive motor neuronopathy depends on the route of delivery. *Ann Neurol* **45:**296–304.
Henderson C (1995) The future for neurotrophic factors as therapeutic agents in neurodegenerative diseases. *Med Sci* **11:**1067–1069.
Henderson CE, Bloch-Gallego E and Camu W (1995) Purified embryonic motoneurons, in *Nerve Cell Culture: A Practical Approach* (Cohen J and Wilkin G eds) pp 69–81, Oxford University Press, London, UK.
Inoue A, Yamakawa J, Yukioka M, and Morisawa S (1983) Filter-binding assay procedure for thyroid hormone receptors. *Anal Biochem* **134:**176–183.
Jacquier A, Buhler E, Schafer MK, Bohl D, Blanchard S, Beclin C, and Haase G (2006) Alsin/Rac1 signaling controls survival and growth of spinal motoneurons. *Ann Neurol* **60:**105–117.
Jamin N, Neumann JM, Ostuni MA, Vu TK, Yao ZX, Murail S, Robert JC, Giatzakis C, Papadopoulos V, and Lacapère JJ (2005) Characterization of the cholesterol recognition amino acid consensus sequence of the peripheral-type benzodiazepine receptor. *Mol Endocrinol* **19:**588–594.
Katzenellenbogen JA, Johnson HJ, Jr., Carlson KE, and Myers HN (1974) Photoreactivity of some light-sensitive estrogen derivatives. Use of an exchange assay to determine their photointeraction with the rat uterine estrogen binding protein. *Biochemistry* **13:**2986–2994.
Lacapère JJ, Delavoie F, Li H, Peranzi G, Maccario J, Papadopoulos V, and Vidic B (2001) Structural and functional study of reconstituted peripheral benzodiazepine receptor. *Biochem Biophys Res Commun* **284:**536–541.
Lacapère JJ and Papadopoulos V (2003) Peripheral-type benzodiazepine receptor: structure and function of a cholesterol-binding protein in steroid and bile acid biosynthesis. *Steroids* **68:**569–585.
Le Fur G, Vaucher N, Perrier ML, Flamier A, Benavides J, Renault C, Dubroeucq MC, Gueremy C, and Uzan A (1983) Differentiation between two ligands for peripheral benzodiazepine binding sites, [^{3}H]RO5–4864 and [^{3}H]PK 11195, by thermodynamic studies. *Life Sci* **33:**449–457.
Lesbordes JC, Cifuentes-Diaz C, Miroglio A, Joshi V, Bordet T, Kahn A, and Melki J (2003) Therapeutic benefits of cardiotrophin-1 gene transfer in a mouse model of spinal muscular atrophy. *Hum Mol Genet* **12:**1233–1239.
Liu J, Lillo C, Jonsson PA, Vande Velde C, Ward CM, Miller TM, Subramaniam JR, Rothstein JD, Marklund S, Andersen PM, et al. (2004) Toxicity of familial ALS-linked SOD1 mutants from selective recruitment to spinal mitochondria. *Neuron* **43:**5–17.
Manfredi G and Xu Z (2005) Mitochondrial dysfunction and its role in motor neuron degeneration in ALS. *Mitochondrion* **5:**77–87.
Massaad C, Coumoul X, Sabbah M, Garlatti M, Redeuilh G, and Barouki R (1998) Properties of overlapping EREs: synergistic activation of transcription and cooperative binding of ER. *Biochemistry* **37:**6023–6032.
McGinnis KM, Gnegy ME, and Wang KK (1999) Endogenous bax translocation in SH-SY5Y human neuroblastoma cells and cerebellar granule neurons undergoing apoptosis. *J Neurochem* **72:**1899–1906.
McGuire V and Nelson LM (2006) Epidemiology of ALS, in *Amyotrophic Lateral Sclerosis* (Mitsumoto H, Przedborski S, and Gordon PH eds) pp 17–41, Taylor & Francis Group, New York.
Michaelidis TM, Sendtner M, Cooper JD, Airaksinen MS, Holtmann B, Meyer M, and Thoenen H (1996) Inactivation of bcl-2 results in progressive degeneration of motoneurons, sympathetic and sensory neurons during early postnatal development. *Neuron* **17:**75–89.
Nelson LM (1995) Epidemiology of ALS. *Clin Neurosci* **3:**327–331.
Oppenheim RW (1989) The neurotrophic theory and naturally occurring motoneuron death. *Trends Neurosci* **12:**252–255.
Oppenheim RW (1996) Neurotrophic survival molecules for motoneurons: an embarrassment of riches. *Neuron* **17:**195–197.
Papadopoulos V, Baraldi M, Guilarte TR, Knudsen TB, Lacapère JJ, Lindemann P, Norenberg MD, Nutt D, Weizman A, Zhang MR, et al. (2006) Translocator protein (18kDa): new nomenclature for the peripheral-type benzodiazepine receptor based on its structure and molecular function. *Trends Pharmacol Sci* **27:**402–409.
Precht TA, Phelps RA, Linseman DA, Butts BD, Le SS, Laessig TA, Bouchard RJ, and Heidenreich KA (2005) The permeability transition pore triggers Bax translocation to mitochondria during neuronal apoptosis. *Cell Death Differ* **12:**255–265.
Pun S, Santos AF, Saxena S, Xu L, and Caroni P (2006) Selective vulnerability and pruning of phasic motoneuron axons in motoneuron disease alleviated by CNTF. *Nat Neurosci* **9:**408–419.
Raucy J, Warfe L, Yueh MF, and Allen SW (2002) A cell-based reporter gene assay for determining induction of CYP3A4 in a high-volume system. *J Pharmacol Exp Ther* **303:**412–423.
Ross TK, Prahl JM, and DeLuca HF (1991) Overproduction of rat 1,25-dihydroxyvitamin D3 receptor in insect cells using the baculovirus expression system. *Proc Natl Acad Sci U S A* **88:**6555–6559.
Sasaki S and Iwata M (1996) Ultrastructural study of synapses in the anterior horn neurons of patients with amyotrophic lateral sclerosis. *Neurosci Lett* **204:**53–56.
Sathasivam S and Shaw PJ (2005) Apoptosis in amyotrophic lateral sclerosis–what is the evidence? *Lancet Neurol* **4:**500–509.
Schilling K and Liao S (1984) The use of radioactive 7 alpha, 17 alpha-dimethyl-19-nortestosterone (mibolerone) in the assay of androgen receptors. *Prostate* **5:**581–588.
Sendtner M, Kreutzberg GW, and Thoenen H (1990) Ciliary neurotrophic factor prevents the degeneration of motor neurons after axotomy. *Nature* **345:**440–441.
Sendtner M, Schmalbruch H, Stockli KA, Carroll P, Kreutzberg GW, and Thoenen H (1992) Ciliary neurotrophic factor prevents degeneration of motor neurons in mouse mutant progressive motor neuronopathy. *Nature* **358:**502–504.
Sheen YY, Ruh TS, Mangel WF, and Katzenellenbogen BS (1985) Antiestrogenic potency and binding characteristics of the triphenylethylene H1285 in MCF-7 human breast cancer cells. *Cancer Res* **45:**4192–4199.
Shoshan-Barmatz V, Israelson A, Brdiczka D, and Sheu SS (2006) The voltage-dependent anion channel (VDAC): function in intracellular signalling, cell life and cell death. *Curr Pharm Des* **12:**2249–2270.
Valenza M, Rigamonti D, Goffredo D, Zuccato C, Fenu S, Jamot L, Strand A, Tarditi A, Woodman B, Racchi M, et al. (2005) Dysfunction of the cholesterol biosynthetic pathway in Huntington's disease. *J Neurosci* **25:**9932–9939.

Address correspondence to: Dr. Thierry Bordet, Trophos, Parc Scientifique de Luminy, Case 931, 13288 Marseille Cedex 9, France. E-mail: tbordet@trophos.com